An 'ideal' form of decaying two-dimensional turbulence

Article

Published Version

J. Fluid Mech. (2002), *vol.* 456, *pp.* 183–198. © 2002 Cambridge University Press
DOI: 10.1017/S0022112001007509 Printed in the United Kingdom

An 'ideal' form of decaying two-dimensional turbulence

By TAKAHIRO IWAYAMA[1]†, THEODORE G. SHEPHERD[1] AND TAKESHI WATANABE[2]

[1]Department of Physics, University of Toronto, Toronto, Ontario M5S 1A7, Canada
[2]Graduate School of Science and Technology, Kobe University, Kobe 657-8501, Japan

(Received 19 March 2001 and in revised form 6 September 2001)

In decaying two-dimensional Navier–Stokes turbulence, Batchelor's similarity hypothesis fails due to the existence of coherent vortices. However, it is shown that decaying two-dimensional turbulence governed by the Charney–Hasegawa–Mima (CHM) equation

$$\frac{\partial}{\partial t}(\nabla^2\varphi - \lambda^2\varphi) + J(\varphi, \nabla^2\varphi) = D,$$

where D is a damping, is described well by Batchelor's similarity hypothesis for wave numbers $k \ll \lambda$ (the so-called AM regime). It is argued that CHM turbulence in the AM regime is a more 'ideal' form of two-dimensional turbulence than is Navier–Stokes turbulence itself.

1. Introduction

The most fascinating characteristic of the two-dimensional Navier–Stokes equations is the existence of two quadratic inviscid invariants, the kinetic energy K and enstrophy Z (half of the mean-square vorticity). The existence of these two invariants leads to the dual cascade phenomenon: an inverse cascade of the kinetic energy and a direct cascade of the enstrophy. In the limit of high Reynolds number, the dissipation of kinetic energy vanishes, while that of enstrophy remains finite. Therefore, Batchelor (1969) hypothesized that the kinetic energy K is the unique invariant of decaying two-dimensional Navier–Stokes turbulence and that the temporal evolution of the system depends only on K and time t. Based on dimensional arguments, he then proposed the self-similar energy spectrum $K(k)$, defined by

$$K = \tfrac{1}{2}\langle \boldsymbol{v}(\boldsymbol{x}) \cdot \boldsymbol{v}(\boldsymbol{x})\rangle = \int_0^\infty K(k)\,\mathrm{d}k, \tag{1.1}$$

as

$$K(k) = K^{3/2} t F(kK^{1/2}t), \tag{1.2}$$

where $\boldsymbol{v}$ is the velocity and F is a universal function, and the angle brackets denote a spatial average. From this follows the decay of enstrophy according to

$$Z = \tfrac{1}{2}\langle \omega(\boldsymbol{x})^2\rangle \sim t^{-2}, \tag{1.3}$$

where ω is the vorticity.

† Permanent affiliation: Graduate School of Science and Technology, Kobe University, Kobe 657-8501, Japan.

However, many direct numerical simulations of decaying two-dimensional Navier–Stokes turbulence have not supported the enstrophy decay law (1.3) (McWilliams 1990; Carnevale *et al.* 1991; Weiss & McWilliams 1993; Chasnov 1997; Bracco *et al.* 2000*b*).† In decaying two-dimensional Navier–Stokes turbulence, long-lived coherent vortices spontaneously emerge from random initial conditions. They evolve through mutual advection, approximately described by Hamiltonian advection of point vortices and the merging of like-signed vortices. Ultimately, they dominate the evolution of the whole system (Fornberg 1977; Basdevant *et al.* 1981; McWilliams 1984; Benzi, Patarnello & Santangelo 1987, 1988). For evolution from a narrow initial energy spectrum, the time evolution of statistical quantities related to the coherent vortices, such as the number of vortices, their mean radius, their mean circulation, etc., is described well by the vortex scaling theory proposed by Carnevale *et al.* (1991). This theory predicts the decay of enstrophy as

$$Z \sim t^{-\xi/2}, \tag{1.4}$$

where ξ is the decay exponent of the number of vortices, and was estimated as $\xi \sim 0.7$–0.75 by numerical simulations and laboratory experiments (Benzi *et al.* 1992; Carnevale *et al.* 1991, 1992; Weiss & McWilliams 1993; Cardoso, Marteau & Tabeling 1994; Siegel & Weiss 1997; Hansen, Marteau & Tabeling 1998; Sire & Chavanis 2000). The scaling exponent ξ was phenomenologically estimated by Iwayama, Fujisaka & Okamoto (1997) as $\xi = 2/3$ by taking into account the Hamiltonian dynamical advection of vortices in the vortex scaling theory of Carnevale *et al.* (1991). They pointed out that the vortex scaling theory is a mean field theory and that fluctuations of vortex statistics cause the observed scaling exponent ξ to deviate from their estimate. In fact, careful analysis of recent high-resolution direct numerical simulations of decaying two-dimensional Navier–Stokes equation performed by Bracco *et al.* (2000*b*) support their estimate. Thus, the decay of enstrophy is found to be much slower than in Batchelor's prediction (1.3). Moreover, there is a disagreement between the time evolution of the spatial scale predicted by the vortex scaling theory and that obtained from (1.2).

The extent of validity of Batchelor's similarity hypothesis for two-dimensional Navier–Stokes turbulence is comprehensively discussed by Bartello & Warn (1996). They note that Batchelor's hypothesis has other implications. Using the assumption that the evolution of the system depends only on K and t, the one-point vorticity probability density function (PDF) is predicted to have the self-similar form

$$p_\omega(\omega, t) \sim t f(\omega t), \tag{1.5}$$

for some symmetric universal function f, and therefore the nth-order moments of the vorticity evolve as

$$\langle |\omega|^n \rangle \sim t^{-n}. \tag{1.6}$$

Direct numerical simulations of decaying two-dimensional Navier–Stokes turbulence performed by Bartello & Warn (1996) showed that (1.6) is valid only for the low-order moments ($n \leqslant 0.4$) and breaks down for the high-order moments: decay rates of high-order moments of the vorticity are constants independent of n, consistent

† Chasnov (1997) investigated the effect of initial Reynolds number $R(0)$ on the decay of enstrophy. He obtained the enstrophy decay law (1.3) only at a critical initial Reynolds number $R(0) = 15.73$. However, the kinetic energy decays as $K \sim t^{-1}$ at this Reynolds number, in contrast to Batchelor's assumption $K \sim t^0$. Thus his result on the enstrophy decay law also does not support Batchelor's prediction.

with the vortex scaling theory. This behaviour arises because the similarity form (1.5) does not hold in the tails of the vorticity PDF, which are hyperbolic but truncated, and which thus control the higher-order moments (including the enstrophy).

The existence of a second asymptotic invariant, ω_{ext}, which is characteristic of the amplitude of the most intense vortices (and is therefore related to the end point of the vorticity PDF), is responsible for the failure of Batchelor's similarity hypothesis. This invariant is inseparably related to the existence of coherent vortices (McWilliams 1990). Therefore, the existence of coherent vortices is the origin of the failure of Batchelor's similarity hypothesis for decaying two-dimensional Navier–Stokes turbulence.

This raises the question of whether there are any two-dimensional turbulent systems for which Batchelor's similarity hypothesis is applicable. In this article, we show that two-dimensional turbulence governed by the Charney–Hasegawa–Mima (CHM) equation in the AM regime $k \ll \lambda$ – equivalently the quasi-geostrophic (QG) potential-vorticity equation for an equivalent-barotropic fluid in the limit of small deformation radius – is described well by Batchelor's similarity hypothesis. This system is very familiar to researchers in the fields of geophysical fluid dynamics and plasma physics.

Two-dimensional turbulence governed by the CHM equation has been actively studied both theoretically and numerically, especially over the past decade (Hasegawa & Mima 1978; Fyfe & Montgomery 1979; Yanase & Yamada 1984; Larichev & McWilliams 1991; Ottaviani & Krommes 1992; Kukharkin, Orszag & Yakhot 1995; Watanabe, Fujisaka & Iwayama 1997; Watanabe, Iwayama & Fujisaka 1998; Iwayama, Watanabe & Shepherd 2001). The equation describes the temporal evolution of quasi-two-dimensional fluctuations of the electrostatic field on the plane perpendicular to a strong magnetic field uniformly applied to a plasma (Hasegawa & Mima 1978). It also describes the temporal evolution of QG motion in geophysical fluids (Pedlosky 1987). The CHM equation in the strong turbulent state neglecting the effects of waves, or equivalently the QG potential vorticity equation on the f-plane, can be written as follows:

$$\frac{\mathrm{D}q}{\mathrm{D}t} \equiv \frac{\partial q}{\partial t} + J(\varphi, q) = D, \tag{1.7a}$$

$$q = \omega - \lambda^2 \varphi, \quad \omega = \nabla^2 \varphi, \tag{1.7b, c}$$

where all quantities are made non-dimensional, $J(\cdot,\cdot)$ is the two-dimensional Jacobian operator, ∇^2 the two-dimensional Laplacian, $\varphi(x, y)$ the electrostatic potential for the plasma case or the variable part of the free surface of the fluid for the geophysical case, and the right-hand side of (1.7a) is a damping term. The constant λ is either the ratio of the horizontal length scale of interest L to the ion Larmor radius in the plasma case, or the ratio of L to the Rossby deformation radius in the geophysical case. Equation (1.7) contains two characteristic regimes. The first is the two-dimensional Navier–Stokes regime that is obtained when $\lambda \to 0$. The governing equation in this regime is the well-known two-dimensional vorticity equation,

$$\frac{\partial \omega}{\partial t} + J(\varphi, \omega) = D. \tag{1.8}$$

The other regime is obtained asymptotically for $\lambda \to \infty$. The governing equation is then

$$\lambda^2 \frac{\partial \varphi}{\partial t} + J(\omega, \varphi) = -D. \tag{1.9}$$

Since (1.9) has been called the asymptotic model (AM) (Larichev & McWilliams 1991), we shall call this regime the AM regime. There are resemblances between turbulent properties of (1.8) and those of (1.7). Equation (1.7) also has two quadratic inviscid invariants: the total energy $\mathsf{E} = -\langle \varphi q \rangle/2$ and the potential enstrophy $\mathsf{Q} = \langle \omega q \rangle/2$. Moreover, a dual cascade (forward cascade of potential enstrophy and inverse cascade of total energy) is possible independent of the value of λ by Fjørtoft's theorem (Fjørtoft 1953), since the total energy spectrum $E(k)$ and the potential enstrophy spectrum $Q(k)$, defined by $\mathsf{E} = \int_0^\infty E(k)\,\mathrm{d}k$ and $\mathsf{Q} = \int_0^\infty Q(k)\,\mathrm{d}k$, respectively, are related by $Q(k) = k^2 E(k)$.

Recently, Watanabe *et al.* (1998) discussed scaling laws for the temporal evolution of a characteristic wavenumber $\bar{k} = \{\int_0^\infty kE(k)\,\mathrm{d}k\}/\mathsf{E}$ and of the energy spectral density at the scale $\bar{k}$ for decaying CHM turbulence in the AM regime. Their discussion is similar to Batchelor's argument for decaying two-dimensional Navier–Stokes turbulence. That is, provided the energy spectrum evolves in a self-similar way and the total energy E is an invariant in the limit of high Reynolds number, the energy spectrum can be expressed as

$$E(k) = \lambda^{-3/4}\mathsf{E}^{9/8}t^{1/4}G(k\lambda^{-3/4}\mathsf{E}^{1/8}t^{1/4}), \tag{1.10}$$

where G is a function of universal form (Watanabe *et al.* 1998). The temporal evolution of the characteristic wavenumber $\bar{k}$ and the energy spectral density at the scale $\bar{k}$ are then

$$\bar{k} \sim t^{-1/4} \quad \text{and} \quad E(\bar{k}) \sim t^{1/4}. \tag{1.11a, b}$$

These results were confirmed by direct numerical simulation of (1.7) evolving from a narrow-band initial energy spectrum. Moreover, self-similarity of the energy spectrum was satisfied well. Furthermore, Watanabe *et al.* (1998) discussed the vortex scaling theory of Carnevale *et al.* (1991) as revised by Iwayama *et al.* (1997), and derived the evolution of the mean vortex radius R_a and the mean distance between vortices l_a as

$$R_a \sim t^{\xi/2} \quad \text{and} \quad l_a \sim t^{\xi/2} \quad \text{with } \xi = \tfrac{1}{2}. \tag{1.12a, b, c}$$

It is possible to consider the length scale corresponding either to the peak of the energy spectrum or to the energy-averaged wavenumber $\bar{k}$ as the mean distance between vortices, because the energy spectrum of decaying CHM turbulence has a single sharp peak. As a result, the vortex scaling theory (1.12*b*, *c*) is consistent with Batchelor's arguments (1.11*a*), in contrast to the case of two-dimensional Navier–Stokes turbulence. Therefore, the results of Watanabe *et al.* (1998) suggest that CHM turbulence in the AM regime is a candidate system for which Batchelor's similarity hypothesis may be applicable.

In this paper, we comprehensively examine the validity of Batchelor's similarity hypothesis for CHM turbulence in order to confirm the above conjecture. For this purpose, we follow the study of Bartello & Warn (1996). That is, the self-similarity of the one-point PDFs of various physical quantities – the stream function φ, the potential vorticity q, the two components of the velocity u and v, and the vorticity ω – and the time evolution of the nth-order moments of these quantities, are examined.

This paper is organized as follows. In § 2, we discuss the implications of Batchelor's similarity hypothesis for CHM turbulence in the AM regime. The self-similar forms of the various PDFs and the temporal scaling laws for the nth-order moments of φ, q, u, v and ω are derived. In § 3, we present results from direct numerical simulations of the CHM equation. The role of coherent vortices vis-à-vis the success of Batchelor's similarity hypothesis is discussed in the concluding § 4.

2. Batchelor's similarity hypothesis for CHM turbulence in the AM regime

In this section, we derive the similarity form of one-point PDFs of the stream function φ, the potential vorticity q, the two components of the velocity $u = -\partial_y \varphi$ and $v = \partial_x \varphi$, and the vorticity ω for CHM turbulence in the AM regime. The temporal exponents of the nth-order moments of these quantities are also derived.

The scale transformations $(x, y) \to a(x, y)$ and $t \to bt$ leave equation (1.9) with $D = 0$ unchanged provided that $\varphi \to \lambda^2 a^4 b^{-1} \varphi$. Therefore the stream function φ in the AM regime is scaled as

$$\varphi \sim \lambda^2 L^4 T^{-1}, \tag{2.1a}$$

where L and T are characteristic scales of length and time, respectively. Since in the AM regime the energy is approximately expressed in terms of φ according to

$$E \approx \tfrac{1}{2}\lambda^2 \langle \varphi^2 \rangle, \tag{2.1b}$$

the length scale L is expressed in terms of E, λ and T as

$$L \sim \lambda^{-3/4} E^{1/8} T^{1/4}. \tag{2.1c}$$

Using relations (2.1) and $E(k) \sim LE$, one obtains the similarity form of the energy spectrum (1.10). The stream function φ, the potential vorticity q, the two components of the velocity u and v, and the vorticity ω are scaled in terms of E, T and λ as follows:

$$\varphi \sim \lambda^{-1} E^{1/2}, \tag{2.2a}$$

$$q \approx -\lambda^2 \varphi \sim \lambda E^{1/2}, \tag{2.2b}$$

$$(u, v) \sim L^{-1} \varphi \sim \lambda^{-1/4} E^{3/8} T^{-1/4}, \tag{2.2c}$$

$$\omega \sim L^{-2} \varphi \sim \lambda^{1/2} E^{1/4} T^{-1/2}. \tag{2.2d}$$

Therefore, the one-point PDFs of φ, q, u, v and ω are predicted to have the self-similar forms

$$p_\varphi(\varphi, t) = \lambda E^{-1/2} g_\varphi(\varphi \lambda E^{-1/2}), \tag{2.3a}$$

$$p_q(q, t) = \lambda^{-1} E^{-1/2} g_q(q \lambda^{-1} E^{-1/2}), \tag{2.3b}$$

$$p_u(u, t) = \lambda^{1/4} E^{-3/8} t^{1/4} g_u(u \lambda^{1/4} E^{-3/8} t^{1/4}), \tag{2.3c}$$

$$p_\omega(\omega, t) = \lambda^{-1/2} E^{-1/4} t^{1/2} g_\omega(\omega \lambda^{-1/2} E^{-1/4} t^{1/2}), \tag{2.3d}$$

for symmetric universal functions g_φ, g_q, g_u and g_ω. The PDF of v is omitted, because the assumption of isotropy of the velocity field yields (2.3c) with v in place of u. The nth-order moments of φ, q, u, v and ω are then obtained from (2.3) as follows under the assumption of isotropy of the velocity field:

$$\langle |\varphi|^n \rangle \sim \lambda^{-n} E^{n/2}, \tag{2.4a}$$

$$\langle |q|^n \rangle \sim \lambda^{n} E^{n/2}, \tag{2.4b}$$

$$\langle |u|^n \rangle = \langle |v|^n \rangle \sim \lambda^{-n/4} E^{3n/8} t^{-n/4}, \tag{2.4c}$$

$$\langle |\omega|^n \rangle \sim \lambda^{n/2} E^{n/4} t^{-n/2}. \tag{2.4d}$$

In order to examine the validity of Batchelor's similarity hypothesis for CHM turbulence in the AM regime, the validity of the self-similar forms of the PDFs (2.3) and the temporal dependence of the nth-order moments (2.4) will be checked by direct numerical simulation of (1.7).

We note that λ in the above discussion is interpreted as L^{-1} in the Navier–Stokes regime. In that case, the above expressions yield Batchelor's similarity spectrum (1.2) and the vorticity and velocity PDFs examined by Bartello & Warn (1996).

3. Numerical simulations

3.1. *Description of simulations*

In this section, we report direct numerical simulations of decaying turbulence governed by (1.7) with the hyperviscosity term $D = -\nu_2 \nabla^4 q$. Also solved is the passive-scalar advection equation,

$$\frac{\mathrm{D}\vartheta}{\mathrm{D}t} = \frac{\partial \vartheta}{\partial t} + J(\varphi, \vartheta) = -\kappa_2 \nabla^4 \vartheta, \tag{3.1}$$

for the purpose of comparison between the potential vorticity q and the passive scalar ϑ. We note that a damping term of the form $D = (-1)^{n-1} \nu_n \nabla^{2n} \omega$ has been used in many previous works (e.g. Larichev & McWilliams 1991; Kukharkin *et al.* 1995; Watanabe *et al.* 1998; Bracco *et al.* 2000*a*; Iwayama *et al.* 2001). However, we adopt the damping term stated above, so that the damping term in the passive-scalar equation (3.1) has the same form as that in the CHM equation (1.7), since q is an advected quantity. The pseudospectral method is used in double precision arithmetic and at resolutions of 256^2 and 512^2, which are the numbers of grid points in the computational domain which has dimensions of $2\pi \times 2\pi$. The aliasing error is suppressed by the 2/3 rule. We set the damping coefficient $\nu_2 = \kappa_2 = 3.0 \times 10^{-8}$ for the low-resolution simulation and $\nu_2 = \kappa_2 = 5.0 \times 10^{-9}$ for the high-resolution simulation. The parameter λ is set at $\lambda = 50$ for the low-resolution simulation and $\lambda = 100$ for the high-resolution simulation. Initial conditions are specified by generating uniform random numbers with a value between 0 and 2π for the phase of each Fourier component of φ. The initial value of the kinetic energy per unit area is normalized to be 0.5. Two initial forms of the energy spectrum, specified by

$$E(k) \propto \frac{k^6}{(k+60)^{18}} \tag{3.2a}$$

or by

$$E(k) \propto \frac{k^{30}}{(k+30)^{60}}, \tag{3.2b}$$

are considered. Both initial spectra have a sharp peak at $k = 30$. The former is frequently used in decaying two-dimensional Navier–Stokes turbulence as a narrow-band spectrum (McWilliams 1990; Weiss & McWilliams 1993; Bracco *et al.* 2000*a*, *b*). The latter is similar to the initial spectra used in Larichev & McWilliams (1991), Watanabe *et al.* (1998), and Iwayama *et al.* (2001). We set the initial value of the passive-scalar field to have the same spectrum as q but with a random phase scrambling so that q and ϑ are initially uncorrelated. Time integration is performed by the Adams–Bashforth scheme with time increments of $\Delta t = 2.5 \times 10^{-3}$ for the low-resolution simulation and $\Delta t = 1.25 \times 10^{-3}$ for the high-resolution simulation. We have checked that the following results are independent of the dissipation term within reasonable limits on ν_2, of the resolution, and of the form of the initial energy spectrum. In what follows we present the results of the high-resolution simulation that have evolved from the spectrum (3.2*a*).

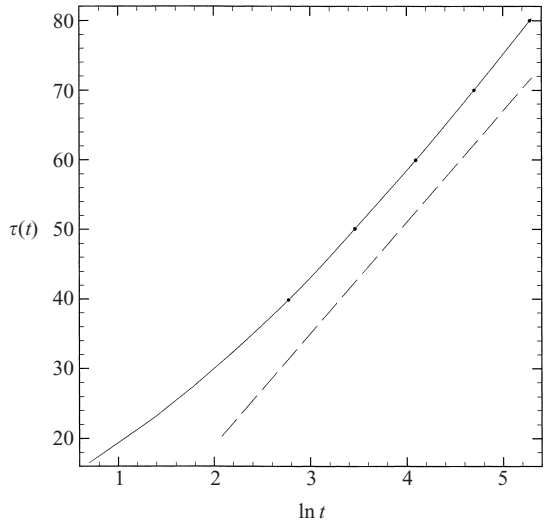

FIGURE 1. Time evolution of the non-dimensional time $\tau(t)$ from (3.3). The dashed line corresponds to the $\ln t$ evolution. The dots indicate the sampling time at which the energy spectra and various PDFs are evaluated.

3.2. *General characterization of the simulation*

Numerical simulations are performed up to $t = 200$. This time corresponds to a non-dimensional time of approximately $\tau = 80$, where τ equals the number of eddy turnover times and is defined by Larichev & McWillams (1991) as

$$\tau(t) = \int_0^t \frac{[2Z(t')]^{1/2}}{1 + (\lambda/\bar{k}_K)^2}\,\mathrm{d}t', \qquad \bar{k}_K \equiv \frac{\displaystyle\int_0^\infty kK(k)\,\mathrm{d}k}{K}. \tag{3.3}$$

When $\lambda = 0$, this definition is equivalent to that commonly used in studies of two-dimensional Navier–Stokes turbulence (e.g. Bartello & Warn 1996; Chasnov 1997). The temporal evolution of the non-dimensional time $\tau(t)$ is found to obey $\tau(t) \sim \ln t$ (figure 1), which is consistent with the simulations of Larichev & McWilliams (1991) and Iwayama *et al.* (2001). The time evolution of $\tau(t)$ can also be derived from Batchelor's similarity argument. Using (1.11*a*) and (2.4*d*) with $n = 2$, the integrand of $\tau(t)$ is scaled in the AM regime as

$$\frac{2Z(t')^{1/2}}{1 + (\lambda/\bar{k}_K)^2} \approx \frac{2}{\lambda^2}\bar{k}_K^2 Z^{1/2} \sim (t')^{-1}. \tag{3.4}$$

Thus, $\tau(t) \sim \ln t$ is obtained theoretically from Batchelor's similarity argument.

We define the dissipation wavenumber as $k_d \equiv \eta^{1/12}\nu_2^{-1/4}$ as in Ohkitani (1991), where η is the potential enstrophy dissipation rate. The dissipation wavenumber k_d algebraically decreases with time from $k_d \simeq 234.8$ at $t = 0$ to $k_d \simeq 117.7$ at $t = 200$ (the figure is omitted). This indicates that the dissipation wavenumber range is sufficiently confined within the high-wavenumber range, due to the adoption of the hyperviscosity term in the evolution equations.

The potential vorticity field q at $t = 196$ ($\tau = 80.0$) is shown in figure 2(*a*). For comparison, the vorticity field ω for decaying two-dimensional Navier–Stokes turbulence ($\lambda = 0$) at $t = 4$ ($\tau = 84.8$) is shown in figure 2(*b*). As seen from the figure,

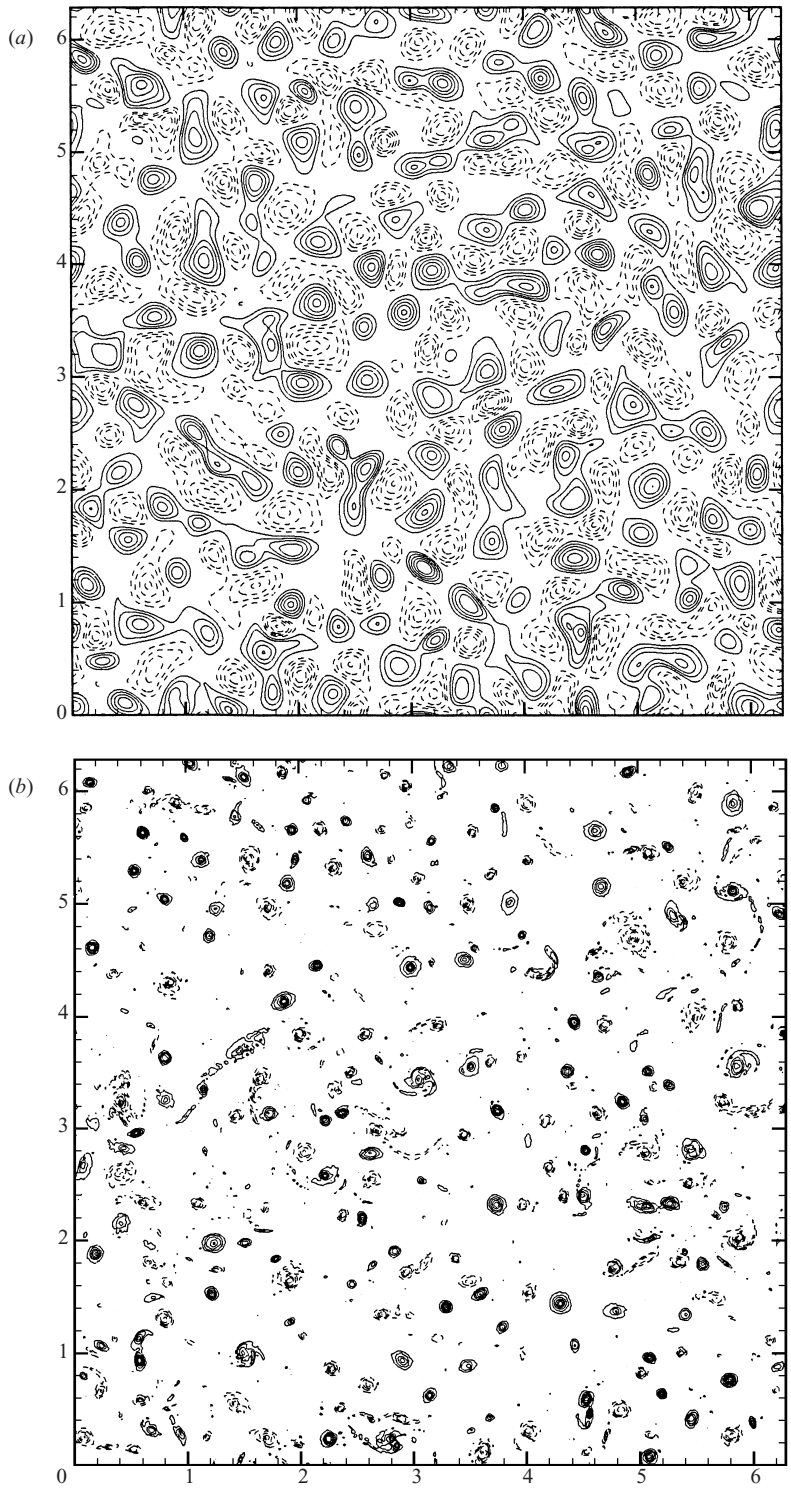

FIGURE 2. (*a*) Potential vorticity q at $t = 196$ ($\tau = 80.0$) for the CHM case and (*b*) vorticity field ω at $t = 4$ ($\tau = 84.8$) for the Navier–Stokes case ($\lambda = 0$). The negative contours are dashed and the zero contour is deleted. The contour intervals are 100 and 15 for (*a*) and (*b*), respectively.

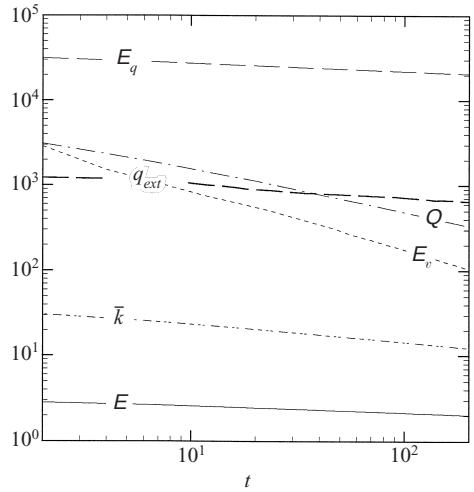

FIGURE 3. Time evolution of half the mean-squared potential vorticity E_q, the potential vorticity extremum q_{ext}, the potential enstrophy Q, the passive scalar variance E_ϑ, the energy-averaged wavenumber $\bar{k}$, and the total energy E.

ω for the Navier–Stokes case has filamentary structure, but q for the CHM case does not, although both fields are governed by the same advection equation.

The evolution of the total energy E, the potential enstrophy Q, the energy-averaged wavenumber $\bar{k}$, the passive-scalar variance

$$E_\vartheta = \tfrac{1}{2}\langle \vartheta^2 \rangle, \tag{3.5}$$

and half the mean-squared potential vorticity

$$E_q = \tfrac{1}{2}\langle q^2 \rangle, \tag{3.6}$$

are shown in figure 3. The decay of all these quantities is algebraic in time. The total energy E is not exactly conserved due to the finiteness of the Reynolds number in this simulation: it decreases from an initial value of 3.19 to a final value of 2.02. However, we can correct for the finiteness of the Reynolds number in the following results by using the instantaneous value of total energy for E in the similarity variables. The characteristic wavenumber $\bar{k}$ decreases algebraically from an initial value of 41.9 to 12.2. Thus, the energy-containing scale of this system belongs to the AM regime. E_q behaves similarly to E, because $E_q = \lambda^2 E + Q \approx \lambda^2 E$ for $\bar{k} \ll \lambda$. The passive-scalar variance E_ϑ decays somewhat faster than the downward cascading quantity Q. In particular, E_ϑ decays while E_q does not, suggesting that in spite of the form of (1.7*a*), q does not filament and develop small scales as it does in two-dimensional Navier–Stokes turbulence. Indeed, this feature can be seen from figure 2.

In order to examine the validity of the self-similar energy spectrum (1.10), the energy spectra at times $t = 16$, 32, 60, 110 and 196 are written in terms of similarity variables using instantaneous total energy (figure 4). These times correspond to $\tau = 39.9$, 50.1, 60.0, 70.0 and 80.0, respectively, i.e. they are approximately equally spaced in terms of τ. It is clear that the energy spectra are collapsing onto a universal functional form with time. Thus Batchelor's similarity argument applied to the energy spectrum of CHM turbulence in the AM regime is verified. The slight deviation from a universal form at the high-wavenumber end of the spectrum might be due to the finite value of λ used in the simulation.

φ	q	u	v	ω
2.69	2.70	3.07	3.10	3.89

TABLE 1. The flatness of various PDFs at $t = 196$.

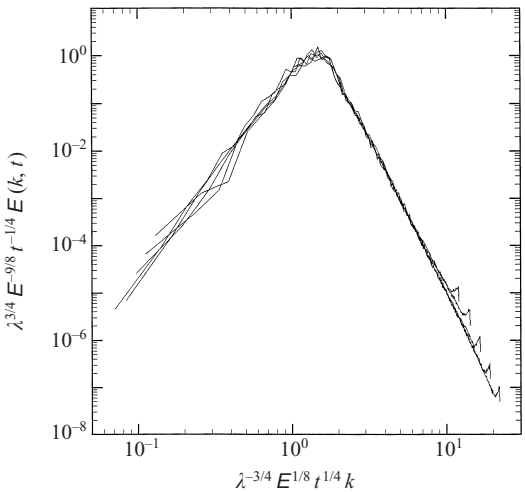

FIGURE 4. Energy spectra at $t = 16$, 32, 60, 110 and 196 in terms of similarity variables.

3.3. *One-point probability densities for various quantities*

In this subsection, further tests of Batchelor's similarity hypothesis are performed by examining the PDFs of φ, q, u, v and ω. Each PDF $p_x(x,t)$ is obtained from the simulation data by counting the number of points $N(x)$ in each field corresponding to the value of x in the interval $(x, x + \delta x)$ and then normalizing $N(x)$ by the total number of grid points. The interval $x_{\min} < x < x_{\max}$ is divided into 400 bins.

The PDFs of φ, q, u, v and ω in terms of similarity variables using instantaneous total energy are shown in figure 5 at the same instants of time as the spectra shown in figure 4. For comparison, the vorticity PDFs for decaying two-dimensional Navier–Stokes turbulence ($\lambda = 0$) are also shown in panel (f). We conclude that all PDFs for CHM turbulence are collapsing onto universal functional forms. In order to specify the various PDFs quantitatively, their flatness is evaluated at $t = 196$ (table 1). Since the potential vorticity can be approximately expressed as $q \approx -\lambda^2\varphi$ in the AM regime, we anticipate that $g_q(\lambda E^{-1/2} q) \approx g_\varphi(-\lambda^{-1} E^{-1/2}\varphi)$. In fact, this relation is satisfied well. The slight deviations of the potential vorticity PDF from the stream function PDF are due to the finite value of λ used in the simulation. The PDFs of u and v are nearly equivalent so the velocity field is statistically isotropic. Moreover, the flatness of the PDFs of u and of v is approximately 3. That is, the velocity PDFs are Gaussian. Recently, Bracco *et al.* (2000*a*) showed from a direct numerical simulation of the CHM equation that the velocity PDF is non-Gaussian. However, the value of λ used in their study was $\lambda = 5$, so their result is likely to be in the Navier–Stokes rather than the AM regime. The vorticity PDF is significantly non-Gaussian, consistent with the results of Larichev & McWilliams (1991). The functional form of the vorticity PDF for the CHM case (figure 5*e*) is very different from that for the Navier–Stokes

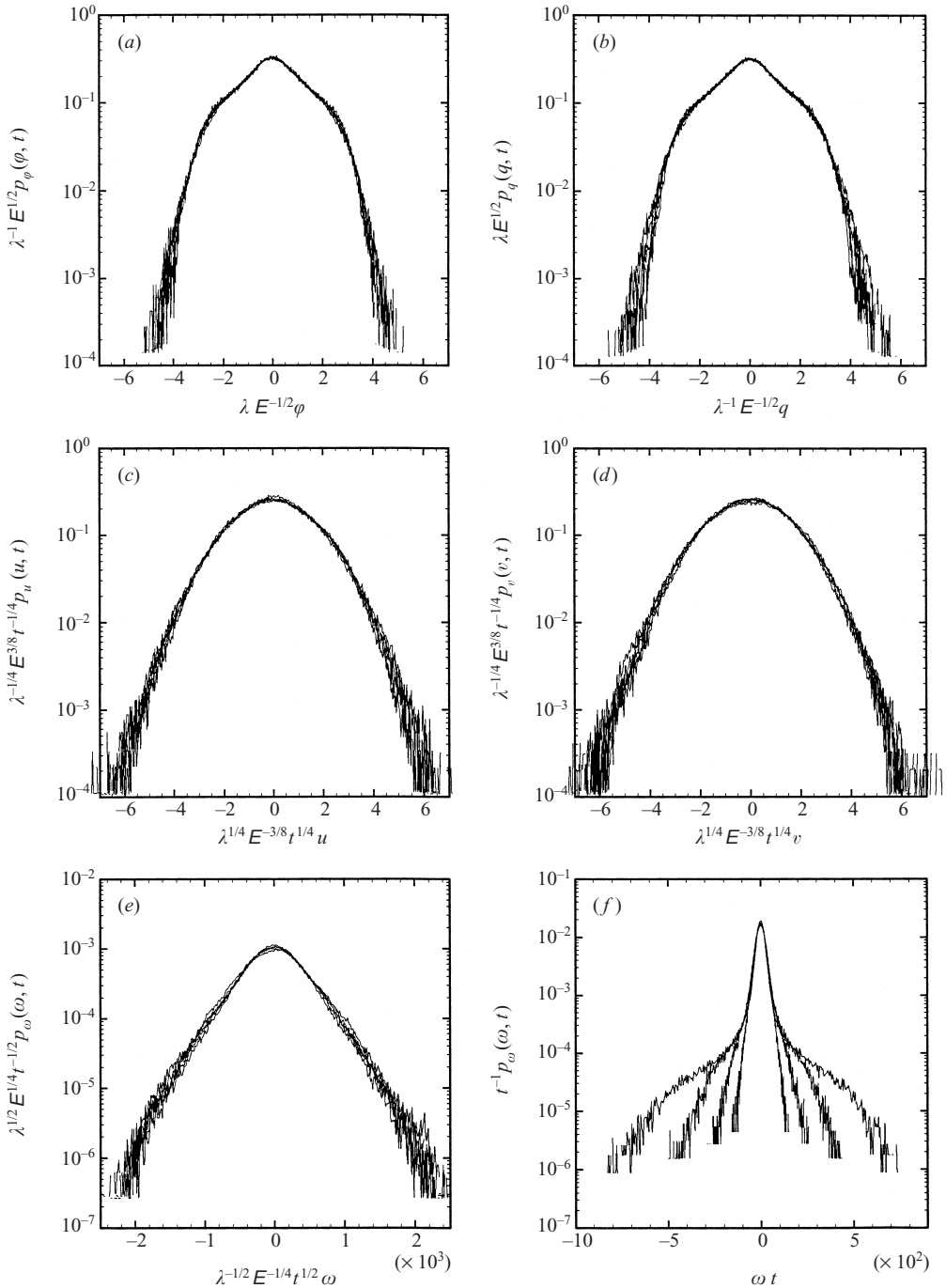

FIGURE 5. PDFs of (*a*) φ, (*b*) q, (*c*) u, (*d*) v, and (*e*) ω at $t = 16$, 32, 60, 110, and 196 in terms of similarity variables. (*f*) The vorticity PDF in terms of similarity variables for the Navier–Stokes case ($\lambda = 0$) at $t = 1.0$, 2.0, 4.0 and 8.0. These times correspond to $\tau = 35.5$, 56.5, 84.8 and 126.6, respectively. The scaled PDF broadens with time in the Navier–Stokes case.

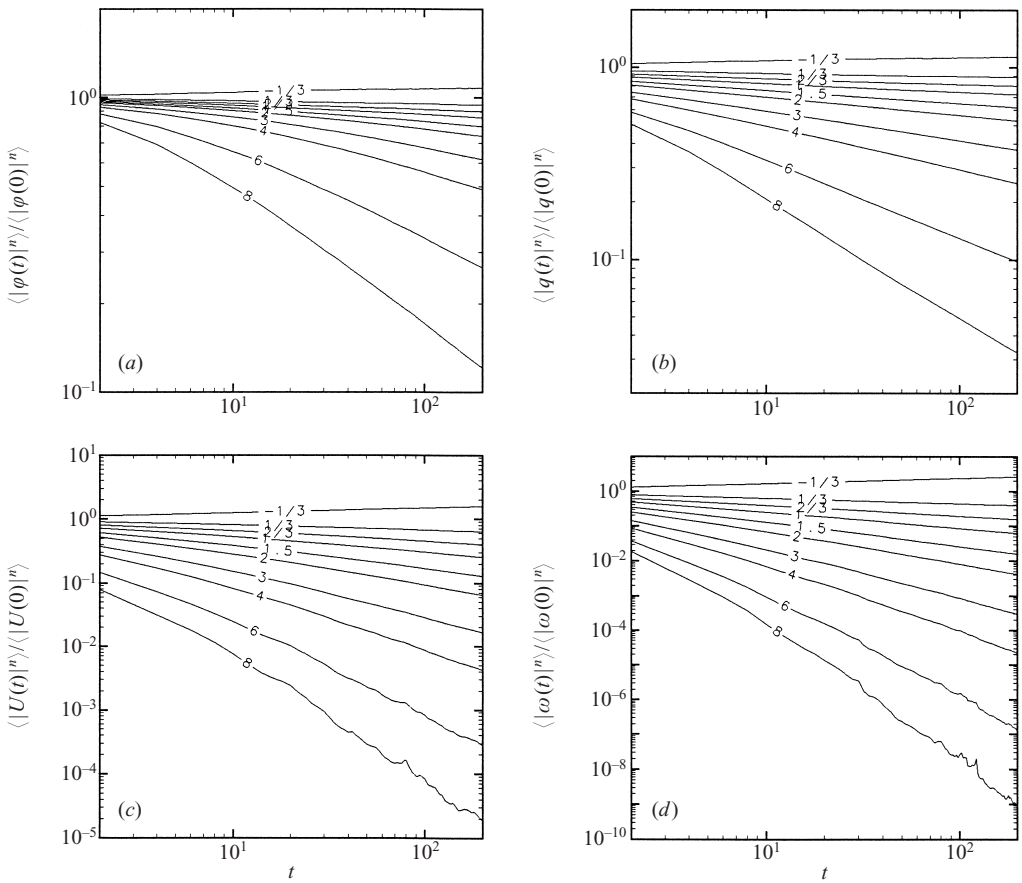

FIGURE 6. Temporal evolution of nth-order moments for (a) φ, (b) q, (c) $U \equiv \sqrt{u^2+v^2}$ and (d) ω for $n = -1/3$, $1/3$, $2/3$, 1, $3/2$, 2, 3, 4, 6 and 8, normalized at $t = 0$.

case (figure 5f). In particular, in the latter case the tails continue to extend outwards with increasing t, as emphasized by Bartello & Warn (1996).

The nth-order moments $\langle|\varphi|^n\rangle$, $\langle|q|^n\rangle$, $\langle|U|^n\rangle$ and $\langle|\omega|^n\rangle$ are analysed from $n = -1/3$ up to $n = 8$ (figure 6), where $U = \sqrt{u^2+v^2}$. Since the velocity field is isotropic, we analyse $\langle|U|^n\rangle$ instead of examining $\langle|u|^n\rangle$ and $\langle|v|^n\rangle$ separately. As shown in figure 6, the temporal development of all moments is algebraic. Thus, the slopes of the moments are evaluated by the least-squares method over the range $20 \leqslant t \leqslant 200$ (figure 7). Also shown are the theoretical results from Batchelor's similarity hypothesis (2.4). We note that the effect of a finite Reynolds number on the slope of the moments, that is, the effect of the slight decrease in energy on the exponents, is eliminated by accounting for the energy dependence on the moments in (2.4). Thus figure 7 indicates the intrinsic temporal exponents of the moments. As expected from figure 5, the numerical results agree well with Batchelor's similarity hypothesis for all orders of moments.

4. Summary and discussion

In decaying two-dimensional Navier–Stokes turbulence, Batchelor's similarity hypothesis describes only the low-order statistics of the vorticity field and breaks down

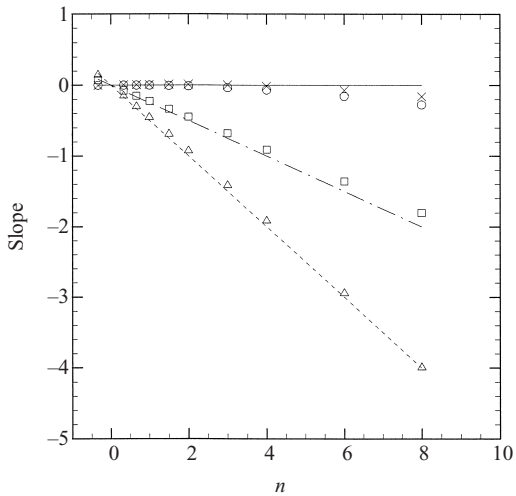

FIGURE 7. Slopes of the moments over the range $20 \leqslant t \leqslant 200$. The solid line, the dash-dot line and the dashed line correspond to predictions from Batchelor's similarity hypothesis (2.4*a*) or equivalently (2.4*b*), (2.4*c*) and (2.4*d*), respectively. The crosses indicate the slopes of $\langle|\varphi|^n\rangle$, the circles $\langle|q|^n\rangle$, the squares $\langle|U|^n\rangle$ and the triangles $\langle|\omega|^n\rangle$.

for the high-order statistics due to the existence of coherent vortices (Bartello & Warn 1996). However, we have shown in this paper that Batchelor's similarity hypothesis works well for decaying CHM turbulence in the AM regime. We derived self-similar forms of the energy spectrum and of the one-point PDFs of various quantities – the stream function, the potential vorticity, the two compoments of velocity, and the vorticity – as well as the time evolution of the nth-order moments of these quantities. We also performed direct numerical simlulations of (1.7) to check the validity of the theoretical estimates. The results of the simulations coincided with the theoretical results. Therefore we conclude that CHM turbulence in the AM regime is a more 'ideal' form of two-dimensional turbulence than is Navier–Stokes turbulence itself.

Larichev & McWilliams (1991) showed that coherent vortices exist even in CHM turbulence in the AM regime. Moreover, Watanabe *et al.* (1998) demonstrated that a vortex scaling theory like that of Carnevale *et al.* (1991) for two-dimensional Navier–Stokes turbulence successfully described the vortex statistics of CHM turbulence in the AM regime. These facts would appear to contradict the success of Batchelor's similarity hypothesis discussed above, because the existence of coherent vortices is responsible for the failure of Batchelor's similarity hypothesis in decaying two-dimensional Navier–Stokes turbulence (Bartello & Warn 1996). Indeed, there are contradictions between the results from Batchelor's similarity hypothesis and the vortex scaling theory in the Navier–Stokes case. Bartello & Warn (1996) generalized Batchelor's similarity theory by taking into account the second asymptotic invariant ω_{ext}, which is characteristic of the amplitude of the most intense vortices, and successfully described the similarity evolution of the energy spectrum.

However, a consistent description of both vortex scaling theory and Batchelor's similarity theory in the case of CHM turbulence in the AM regime is possible, as follows. Although the potential vorticity of the core of the most intense vortex, q_{ext}, is an approximate invariant (figure 3), the total energy E and q_{ext} cannot be treated as independent invariants. This is because the self-similarity of the potential vorticity PDF (figure 5*b*) means that q_{ext} is related to E_q, while E_q reduces to the total energy,

$E_q = \langle |q|^2 \rangle / 2 \approx \lambda^2 E$, in the AM regime, as mentioned in § 3.2. Therefore, there are no additional invariants beyond the total energy E for CHM turbulence in the AM regime. As a result, it is possible to reconcile Batchelor's similarity theory with the vortex scaling theory.

The self-similarity of the potential vorticity PDF and, in particular, its well-behaved tails, raises the question of whether the vortices in the AM regime of CHM turbulence really are 'coherent'. Certainly there is nothing reminiscent of the strong intermittency of the vorticity field exhibited in two-dimensional Navier–Stokes turbulence; the vortices of the AM regime of CHM turbulence are more like a quasi-crystal (Kukharkin *et al.* 1995), rather than a collection of independent, individual entities. It is the strong intermittency of the vorticity field in two-dimensional Navier–Stokes turbulence, reflected in the non-self-similar tails of the vorticity PDF, that leads to the deviations from Batchelor's similarity theory identified by Bartello & Warn (1996). In contrast, the AM regime of CHM turbulence obeys Batchelor's similarity theory because of the absence of intermittency. Although vortices exist, they are not particularly special objects and presumably their evolution cannot be understood in terms of the dynamics of point vortices, as in two-dimensional Navier–Stokes turbulence.

A natural question is why it is that CHM turbulence in the AM regime exhibits no intermittency. This paper does not attempt to address this question. However, it may be noted that two-dimensional Navier–Stokes turbulence (1.8) involves advection of $\nabla^2\varphi$ by φ, i.e. by the larger scales of motion, and this leads to the long-range, persistent straining that is reflected in filamentary structures and non-Gaussian statistics (long tails). In contrast, CHM turbulence in the AM regime (1.9) involves advection of φ by $\nabla^2\varphi$, i.e. by the smaller scales of motion, and this may be expected to lead to more 'random walk' behaviour and to suppress intermittency. The contrast between these two behaviours is evident in the physical-space fields shown in figure 2. However, these ideas remain at this stage purely speculative.

We have shown that Batchelor's similarity hypothesis describes well not only the lower order but also the higher order statistics of CHM turbulence in the AM regime. This similarity behaviour cannot be modelled by a closure model, because it is valid only at the second-order moment. However, the lack of intermittency evident in the PDFs suggests that a closure model stands a much better chance of representing the second-order statistics of CHM turbulence in the AM regime than those of two-dimensional Navier–Stokes turbulence, where the failures have been well documented (e.g. Herring & McWilliams 1985). To address this question it would be interesting to compare results of direct numerical simulations with those of closure calculations. This point should be the subject of a future study.

It is natural to ask whether there are other decaying two-dimensional turbulent systems for which Batchelor's similarity hypothesis is applicable. Pierrehumbert, Held & Swanson (1994) proposed a family of models of two-dimensional turbulence, so-called α-turbulence, governed by

$$\frac{\partial q}{\partial t} + J(\varphi, q) = 0, \tag{4.1a}$$

$$\hat{\varphi}(\boldsymbol{k}) = -|\boldsymbol{k}|^{-\alpha}\hat{q}(\boldsymbol{k}), \tag{4.1b}$$

where $\hat{\varphi}(\boldsymbol{k})$ and $\hat{q}(\boldsymbol{k})$ are the Fourier coefficients of φ and q with wavenumber $\boldsymbol{k}$, respectively. This equation reduces to the vorticity equation of the inviscid Navier–Stokes system for $\alpha = 2$, and to the surface quasi-geostrophic equation for $\alpha = 1$. The CHM equation in the AM regime corresponds to $\alpha = -2$. Recently, α-turbulence

has attracted much research interest and it is under active study (Held *et al.* 1995; Ohkitani & Yamada 1997; Schorghofer 2000*a*, *b*). However, the previous studies on α-turbulence have studied only the positive-α regime. The present study suggests the need to study the negative-α regime.

This work was made possible during a visit by T. I. to the Physics Department at the University of Toronto, which was supported by the Ministry of Education, Culture, Sports, Science and Technology of Japan. T. I. expresses his deep thanks to all the members of the T. G. S. group for many stimulating discussions, encouragement and hospitality during his visit. The GFD-DENNOU Library was used for drawing figures.

REFERENCES

Bartello, P. & Warn, T. 1996 Self-similarity of decaying two-dimensional turbulence. *J. Fluid Mech.* **326**, 357–372.

Basdevant, C., Legras, B., Sadourny, R. & Béland, M. 1981 A study of barotropic model flows: intermittency, waves and predictability. *J. Atmos. Sci.* **38**, 2305–2326.

Batchelor, G. K. 1969 Computation of the energy spectrum in homogeneous two-dimensional turbulence. *Phys. Fluids Suppl.* **12**, II-233–II-239.

Benzi, R., Colella, M., Briscolini, M. & Santangelo, P. 1992 A simple point vortex model for two-dimensional decaying turbulence. *Phys. Fluids* A **4**, 1036–1039.

Benzi, R., Patarnello, S. & Santangelo, P. 1987 On the statistical properties of two-dimensional decaying turbulence. *Europhys. Lett.* **3**, 811–818.

Benzi, R., Patarnello, S. & Santangelo, P. 1988 Self-similar coherent structures in two-dimensional decaying turbulence. *J. Phys.* A: *Math. Gen.* **21**, 1221–1237.

Bracco, A., LaCasce, J., Pasquero, C. & Provenzale, A. 2000*a* The velocity distribution of barotropic turbulence. *Phys. Fluids* **12**, 2478–2488.

Bracco, A., McWilliams, J. C., Murante, G., Provenzale, A. & Weiss, J. B. 2000*b* Revisiting freely decaying two-dimensional turbulence at millennial resolution. *Phys. Fluids* **12**, 2931–2941.

Cardoso, O., Marteau, D. & Tabeling, P. 1994 Quantitative experimental study of the free decay of quasi-two-dimensional turbulence. *Phys. Rev.* E **49**, 454–461.

Carnevale, G. F., McWilliams, J. C., Pomeau, Y., Weiss, J. B. & Young, W. R. 1991 Evolution of vortex statistics in two-dimensional turbulence. *Phys. Rev. Lett.* **66**, 2735–2737.

Carnevale, G. F., McWilliams, J. C., Pomeau, Y., Weiss, J. B. & Young, W. R. 1992 Rates, pathways, and end states of nonlinear evolution in decaying two-dimensional turbulence: Scaling theory versus selective decay. *Phys. Fluids* A **4**, 1314–1316.

Chasnov, J. R. 1997 On the decay of two-dimensional homogeneous turbulence. *Phys. Fluids* **9**, 171–180.

Fjørtoft, R. 1953 On the changes in the spectral distribution of kinetic energy for two-dimensional non-divergent flow. *Tellus* **5**, 225–230.

Fornberg, B. 1977 A numerical study of two-dimensional turbulence. *J. Comput. Phys.* **25**, 1–31.

Fyfe, D. & Montgomery, D. 1979 Possible inverse cascade behavior for drift-wave turbulence. *Phys. Fluids* **22**, 246–248.

Hansen, A. E., Marteau, D. & Tabeling, P. 1998 Two-dimensional turbulence and dispersion in a freely decaying system. *Phys. Rev* E **58**, 7261–7271.

Hasegawa, A. & Mima, K. 1978 Pseudo-three-dimensional turbulence in magnetized nonuniform plasma. *Phys. Fluids* **21**, 87–92.

Held, I. M., Pierrehumbert, R. T., Garner, S. T. & Swanson, K. L. 1995 Surface quasi-geostrophic dynamics. *J. Fluid Mech.* **282**, 1–20.

Herring, J. R. & McWilliams, J. C. 1985 Comparison of direct numerical simulation of two-dimensional turbulence with two-point closure: the effects of intermittency. *J. Fluid Mech.* **153**, 229–242.

Iwayama, T., Fujisaka, H. & Okamoto, H. 1997 Phenomenological determination of scaling exponents in two-dimensional decaying turbulence. *Prog. Theor. Phys.* **98**, 1219–1224.

Iwayama, T., Watanabe, T. & Shepherd, T. G. 2001 Infrared dynamics of decaying two-dimensional turbulence governed by the Charney–Hasegawa–Mima equation. *J. Phys. Soc. Japan* **70**, 376–386.

Kukharkin, N., Orszag, S. A. & Yakhot, V. 1995 Quasicrystallization of vortices in drift-wave turbulence. *Phys. Rev. Lett.* **75**, 2486–2489.

Larichev, V. D. & McWilliams, J. C. 1991 Weakly decaying turbulence in an equivalent-barotropic fluid. *Phys. Fluids* A **3**, 938–950.

McWilliams, J. C. 1984 The emergence of isolated coherent vortices in turbulent flow. *J. Fluid Mech.* **146**, 21–43.

McWilliams, J. C. 1990 The vortices of two-dimensional turbulence. *J. Fluid Mech.* **219**, 361–385.

Ohkitani, K. 1991 Wave number space dynamics of enstrophy cascade in a forced two-dimensional turbulence. *Phys. Fluids* A **3**, 1598–1611.

Ohkitani, K. & Yamada, M. 1997 Inviscid and inviscid-limit behavior of a surface quasigeostrophic flow. *Phys. Fluids* **9**, 876–882.

Ottaviani, M. & Krommes, J. A. 1992 Weak- and strong-turbulence regimes of the forced Hasegawa–Mima equation. *Phys. Rev. Lett.* **69**, 2923–2926.

Pedlosky, J. 1987 *Geophysical Fluid Dynamics*, 2nd Edn. Springer.

Pierrehumbert, R. T., Held, I. M. & Swanson, K. 1994 Spectra of local and nonlocal two-dimensional turbulence. *Chaos, Solitons and Fractals* **4**, 1111–1116.

Schorghofer, N. 2000*a* Universality of probability distributions among two-dimensional turbulent flows. *Phys. Rev.* E **61**, 6568–6571.

Schorghofer, N. 2000*b* Energy spectra of steady two-dimensional turbulent flows. *Phys. Rev.* E **61**, 6572–6577.

Siegel, A. & Weiss, J. B. 1997 A wavelet-packet census algorithm for calculating vortex statistics. *Phys. Fluids* **9**, 1988–1999.

Sire, C. & Chavanis, P.-H. 2000 Numerical renormalization group of vortex aggregation in two-dimensional decaying turbulence: The role of three-body interactions. *Phys. Rev.* E **61**, 6644–6653.

Watanabe, T., Fujisaka, H. & Iwayama, T. 1997 Dynamical scaling law in the development of drift wave turbulence. *Phys. Rev.* E **55**, 5575–5580.

Watanabe, T., Iwayama, T. & Fujisaka, H. 1998 Scaling law for coherent vortices in decaying drift Rossby wave turbulence. *Phys. Rev.* E **57**, 1636–1643.

Weiss, J. B. & McWilliams, J. C. 1993 Temporal scaling behavior of decaying two-dimensional turbulence. *Phys. Fluids* A **5**, 608–621.

Yanase, S. & Yamada, M. 1984 The effect of the finite Rossby radius on two-dimensional isotropic turbulence. *J. Phys. Soc. Japan* **53**, 2513–2520.